Identification of the Catalytic Base in Long Chain Acyl-CoA Dehydrogenase†

Snezana Djordjevic,‡,§ Yu Dong,§,∥ Rosemary Paschke,‡ Frank E. Frerman,⊥ Arnold W. Strauss,∥ and Jung-Ja P. Kim*,‡

Department of Biochemistry, Medical College of Wisconsin, Milwaukee, Wisconsin 53226, Departments of Pediatrics and Molecular Biology and Pharmacology, Washington University School of Medicine, St. Louis, Missouri 63110, and Department of Pediatrics, University of Colorado School of Medicine, Denver, Colorado 80262

Received October 13, 1993; Revised Manuscript Received February 4, 1994®

ABSTRACT: We have used molecular modeling and site-directed mutagenesis to identify the catalytic residues of human long chain acyl-CoA dehydrogenase. Among the acyl-CoA dehydrogenases, a family of flavoenzymes involved in β-oxidation of fatty acids, only the three-dimensional structure of the medium chain fatty acid specific enzyme from pig liver has been determined (Kim, J.-J. P., Wang, M., & Paschke, R. (1993) *Proc. Natl. Acad. Sci. U.S.A. 90,* 7523–7527). Despite the overall sequence homology, the catalytic residue (E376) of medium chain acyl-CoA dehydrogenase is not conserved in isovaleryl- and long chain acyl-CoA dehydrogenases. A molecular model of human long chain acyl-CoA dehydrogenase was derived using atomic coordinates determined by X-ray diffraction studies of the pig medium chain specific enzyme, interactive graphics, and molecular mechanics calculations. The model suggests that E261 functions as the catalytic base in the long-chain dehydrogenase. An altered dehydrogenase in which E261 was replaced by a glutamine was constructed, expressed, purified, and characterized. The mutant enzyme exhibited less than 0.02% of the wild-type activity. These data strongly suggest that E261 is the base that abstracts the α-proton of the acyl-CoA substrate in the catalytic pathway of this dehydrogenase.

The first step in the β-oxidation of fatty acids in mammalian mitochondria is catalyzed by a family of flavoproteins, the acyl-CoA[1] dehydrogenases. The reaction mechanism involves base-catalyzed α-proton abstraction from the acyl-CoA substrate, followed by the transfer of the β-hydride to the N(5) position of the enzyme-bound flavin adenine dinucleotide (FAD) (Thorpe *et al.*, 1981; Ghisla *et al.*, 1984). Three distinct soluble enzymes, specific for straight chain fatty acyl-CoA thioesters, have been isolated from mammalian mitochondria (Beinert, 1963; Ikeda *et al.*, 1985). These enzymes are homotetramers, with each subunit containing about 400 amino acid residues and one FAD. These dehydrogenases differ in their substrate specificities. For example, in rat liver mitochondria short chain acyl-CoA dehydrogenase (SCAD) exhibits optimal activity (V_{max}/K_m) with butanoyl CoA (C_4-CoA), medium chain acyl-CoA dehydrogenase (MCAD) exhibits optimal activity with octanoyl CoA (C_8-CoA), and long chain acyl-CoA dehydrogenase (LCAD) exhibits optimal activity with palmitoyl CoA (C_{16}-CoA) as a substrate (Ikeda *et al.*, 1985). cDNAs encoding the rat and human enzymes have been cloned and sequenced (Naito *et al.*, 1989; Kelly *et al.*, 1987; Indo *et al.*, 1992; Matsubara *et al.*, 1989). Recently, a very long chain acyl-CoA dehydrogenase (VLCAD) has been identified, which is loosely bound to the inner membrane of rat liver mitochondria (Izai *et al.*, 1992). This enzyme is a homodimer, and each 71-kDa subunit contains one FAD. VLCAD's substrate specificity and immunochemical properties differ from those of the soluble acyl-CoA dehydrogenases.

During the last decade, acyl-CoA dehydrogenase deficiencies have been recognized as genetic disorders that are linked with numerous symptoms. LCAD-deficient patients suffer from hypoglycemia, vomiting, coma, and skeletal and cardiac muscle hypertrophy (Roe & Coates, 1989). These findings have prompted an increased interest in studying the structure and enzyme mechanisms of these flavoenzymes. Chemical modification experiments using a mechanism-based inhibitor (2-octynoyl-CoA) suggested that E376 of MCAD was the α-proton-abstracting base that initiates the dehydrogenation reaction (Powell & Thorpe, 1988). The three-dimensional structure of pig MCAD and its complex with a substrate have been determined to 2.4-Å resolution by X-ray diffraction methods (Kim *et al.*, 1993). The structural analysis of the complex identified E376 in the substrate binding site at an appropriate distance and orientation to abstract the α-proton from the substrate. The human wild-type and E376Q mutant MCADs were expressed and characterized (Bross *et al.*, 1990). The E376Q mutant retained less than 0.02% of the activity of the wild-type enzyme, consistent with E376 acting as the catalytic base.

Sequence alignment of the short, medium, and long chain specific enzymes indicates significant homology spanning the entire polypeptide chain (Indo *et al.*, 1991; Matsubara *et al.*, 1989). Despite the high sequence homology, a glutamate residue is not conserved in LCAD at the position corresponding to E376 of MCAD and SCAD (Figure 1). The primary sequence alignment shows that, in the long chain specific

† This research was supported by Research Grants GM29076 (J.-J.P.K.), AM20407 (A.W.S.), and HD08315 (F.E.F.) from the National Institutes of Health.

* To whom correspondence should be addressed.
‡ Medical College of Wisconsin.
§ The first two authors contributed equally to the work.
∥ Washington University School of Medicine.
⊥ University of Colorado School of Medicine.

® Abstract published in *Advance ACS Abstracts,* March 15, 1994.

[1] Abbreviations: FAD, flavin adenine dinucleotide; CoA, coenzyme A; MCAD, medium chain acyl-CoA dehydrogenase; SCAD, short chain acyl-CoA dehydrogenase; LCAD, long chain acyl-CoA dehydrogenase; IVD, isovaleryl-CoA dehydrogenase; VLCAD, very long chain acyl-CoA dehydrogenase; ETF, electron-transfer flavoprotein; PCR, polymerase chain reaction; Tris, tris(hydroxymethyl)aminomethane; DEAE, diethylaminoethyl; SDS–PAGE, sodium dodecyl sulfate–polyacrylamide gel electrophoresis; kDa, kilodalton(s); DCPIP, 2,6-dichlorophenolindophenol; PMS, phenazine methosulfate; C_4-CoA, butanoyl-CoA; C_8-CoA, octanoyl-CoA; C_{10}-CoA, decanoyl-CoA; C_{12}-CoA, dodecanoyl-CoA; C_{16}-CoA, palmitoyl-CoA.

0006-2960/94/0433-4258$04.50/0

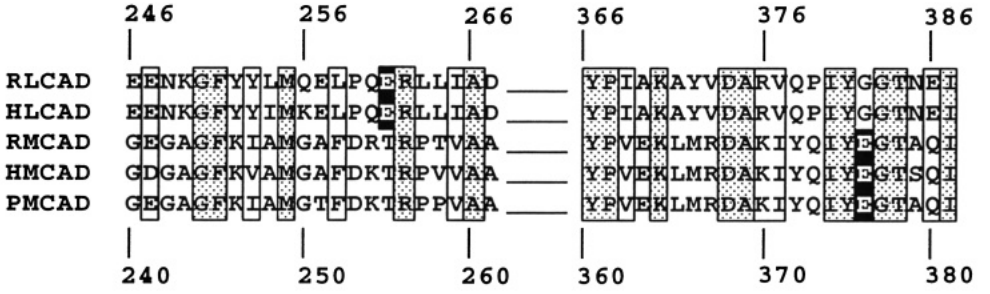

FIGURE 1: A portion of the sequence alignment of rat (R) and human (H) LCAD and rat, human, and pig (P) MCAD. The numbers above the sequences correspond to LCAD, whereas the numbers below the sequences correspond to the mature form of the MCAD enzymes. Only the segments around LCAD residues 261 and 382 are shown. Identical residues are indicated by stippled boxes; unstippled boxes indicate similar regions; the catalytic residues are labeled with white letters on a black background.

dehydrogenase, the amino acid residue at the position corresponding to the catalytic base (382 in the LCAD sequence), glutamate 376 in MCAD, is a glycine. In the amino acid sequence of rat IVD, there is also a glycine in this position, whereas human IVD contains an alanine (Matsubara *et al.*, 1990). It is not apparent from the primary structure of LCAD which other residue could play the role of E376 in MCAD. This consideration raised doubts about the catalytic role of E376 in MCAD (Indo *et al.*, 1991).

Primary sequence comparison was insufficient to identify either the residues involved in substrate binding and specificity or the active site base. In the absence of a three-dimensional structure, we have approached the problem of identifying these residues in LCAD by combining the methods of computer modeling and site-directed mutagenesis. Preliminary results of the modeling were reported previously (Kim *et al.*, 1992). The most striking feature of the model is that the carboxylate of E261 in LCAD (residue T255 in the MCAD sequence) corresponds to the E376 carboxylate from MCAD. Thus, E261 is the most likely candidate for initiating the dehydrogenation reaction. Wild-type human LCAD has been cloned, expressed in *Escherichia coli* and characterized (unpublished results). We report our first attempt toward identifying functional residues in this enzyme. We have constructed, expressed, purified, and characterized an altered human LCAD protein where glutamine was substituted for E261.

EXPERIMENTAL PROCEDURES

In Vitro Mutagenesis and Construction of the Expression Plasmid for Mutant Human LCAD. The plasmid pETLCAD contains only the coding sequence for mature human LCAD subcloned into the pET-11a (Novagen) expression vector at *Nde*I and *Nhe*I sites. Details of the cloning procedures and the construction of the expression plasmid for wild-type HLCAD will be described elsewhere. The active site mutant DNA of human LCAD was generated by an extension of overlapping mutant DNA sequences by the polymerase chain reaction (PCR) using pETLCAD as the template. The two mutagenesis primers (5′-CTTCCACAGCAAAGGCTGTTA-3′) created a G to C transition at nucleotide position 781 (underlined), resulting in substitution of glutamine for E261. The two extension primers were T7 promoter and T7 terminator purchased from Novagen. One hundred micrograms of the template DNA was amplified by 30 PCR cycles in 100 μL of a reaction mixture containing 10 mM Tris-HCl, pH 8.3, 100 mM KCl, 2.5 mM $MgCl_2$, 10 mM dithiothreitol, 200 μM of each deoxynucleotide triphosphate, 100 pmol of both the 5′ and 3′ primers, and 2.5 units of Taq polymerase (Perkin Elmer). Each cycle was programmed as follows: 94 °C, 1 min; 55 °C, 1 min; 72 °C, 1 min. The final PCR product was double digested with *Nde*I and *Nhe*I and subcloned into pET-11a to obtain plasmid pETLCAD/E261Q. The expression plasmids, both the wild-type and the mutant, were sequenced in their entirety to assure that no errors secondary to the PCR were created. The NH_2-terminal sequence of the wild-type protein matches the expected sequence predicted by the cDNA as expressed.

Purification of the Expressed E261Q Mutant of Human LCAD. The purification procedure for the E261Q mutant was essentially the same as that used to purify the wild-type enzyme. Harvested cells were sonicated in a buffer containing 20 mM Tris-HCl, pH 8.0, 50 mM sucrose, and 10 mM EDTA. Broken cells were then centrifuged for 1 h at 70000*g*. The supernatant was fractionated with ammonium sulfate. The fraction between 40 and 80% saturation of ammonium sulfate was dialyzed in 50 mM potassium phosphate, pH 7.0, and loaded on a DEAE-cellulose column. LCAD binds weakly to the DEAE, and it was eluted with a 50–100 mM phosphate gradient. The fractions containing LCAD were pooled and further separated on a Sepharose Q column (Pharmacia), using a 50–350 mM phosphate gradient at pH 7.0 containing 10% glycerol. The last step of purification was achieved by hydroxylapatite chromatography using a 50–350 mM phosphate gradient, pH 7.0. The enzyme fractions were followed by UV–vis absorbance and SDS–PAGE. Protein concentrations were determined by using the Bio-Rad protein assay (Bradford, 1976).

Enzyme Assay. Acyl-CoA dehydrogenase activity was followed spectrophotometrically, by using 2,6-dichlorophenolindophenol (DCPIP) as the terminal electron acceptor (Crane *et al.*, 1956; Ikeda *et al.*, 1985), by the ferricenium assay (Lehman & Thorpe, 1990), or by following the decrease in fluorescence of electron-transfer flavoprotein (ETF) (Beckman & Frerman, 1983). The reaction was initiated by addition of the purified enzyme or, when crude cell extract was being assayed, by addition of the fatty acyl-CoA substrates (Sigma). In the assay with DCPIP, we used either 3 mM phenazine methosulfate (PMS) or 5 μM pig liver ETF as the intermediate electron acceptor. Reactions were monitored on a Cary-219 or a Shimadzu UV-160 spectrophotometer. Fluorescence measurements were made with a Perkin-Elmer LS-5 fluorometer.

Anaerobic Substrate Addition. Anaerobic conditions were maintained by the following method. The enzyme in buffer (50 mM phosphate, pH 7.5, and 10% glycerol) and acyl-CoA solutions were stored for 3–4 h in a Coy anaerobic chamber. The anaerobic chamber was equipped with an oxygen analyzer sensitive to 2 ppm. In this chamber, lumiflavin remained reduced for over 42 h, indicating that the oxygen content in the chamber was negligible. Inside the chamber, LCAD was transferred to a silicated quartz cuvette, which was then

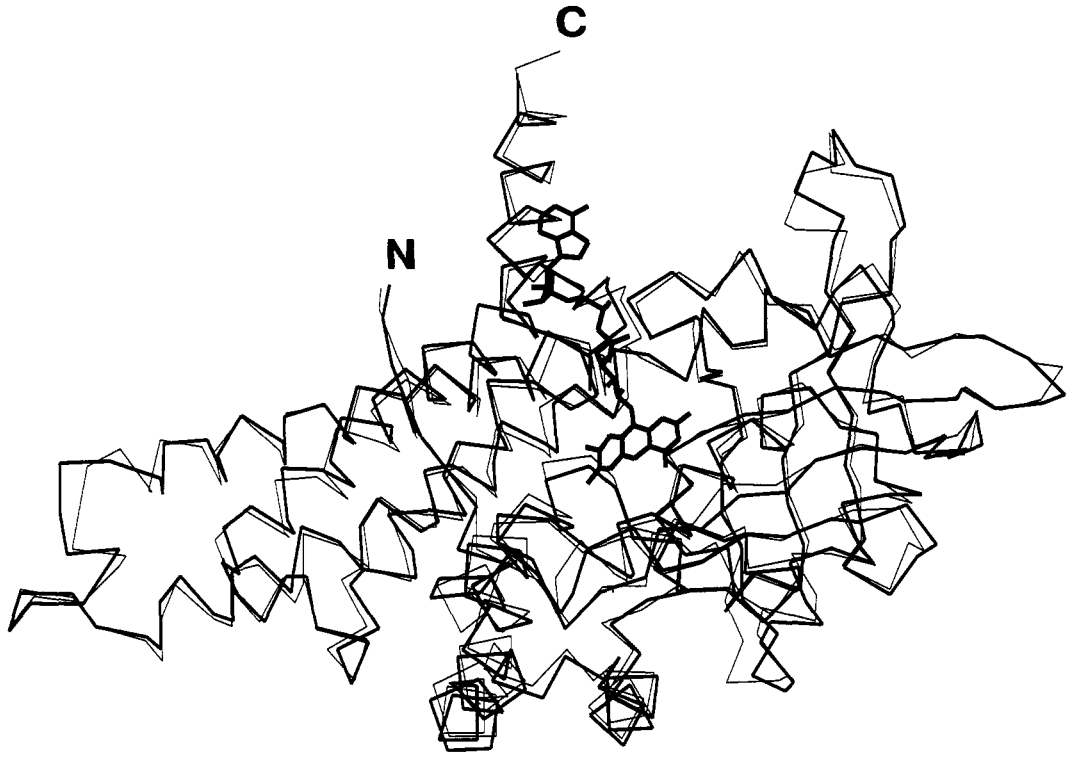

FIGURE 2: Comparison of the overall Cα-fold of the modeled human LCAD and the X-ray structure of pig MCAD. Minor changes in the backbone atom positions of MCAD (thin line) were sufficient for accommodating side chains of LCAD (medium line). N- and C-terminal ends are indicated. FAD is represented by thick lines.

capped. The spectrum of the ligand-free oxidized enzyme was recorded using a Cary-219 or Shimadzu UV-160 spectrophotometer. Subsequent additions of substrate were made inside the anaerobic chamber.

Molecular Modeling of Human LCAD. Long chain acyl-CoA dehydrogenase was modeled on the basis of its sequence homology to pig MCAD for which a 2.4-Å crystal structure has been determined and refined (Kim *et al.*, 1993). Side-chain replacements were made on the basis of a multiple sequence alignment similar to that previously generated (Indo *et al.*, 1991). In our alignment, there were no gaps between LCAD residues 85 and 155, whereas the same region contained a single deletion and an insertion in the alignment reported by Indo *et al.* The starting model of the LCAD backbone was constructed by keeping the coordinates from the MCAD structure except for a single deletion in the loop region after residue 196. The shorter loop caused by the deletion was manually modeled using the computer graphics program FRODO (Cambillau & Horjales, 1987) on a Silicon Graphics IRIS personal work station. The atomic coordinates for the side chains of the LCAD starting model were assigned from the MCAD structure when the residues of the two polypeptides were identical. When a side chain of LCAD was smaller than the corresponding side chain of MCAD, the atomic coordinates for the smaller side chain were derived from the coordinates of the equivalent atoms within the larger side chain. When a side chain of LCAD was larger than the side chain of MCAD, only the coordinates for the atoms common to both side chains were used in the starting model. The resulting coordinates were used as input to AMBER 3a, a computer model building program (Weiner & Kollman, 1981; Weiner *et al.*, 1986). All of the missing atomic coordinates for the larger side chains were assigned by the EDIT module of AMBER which uses standard amino acids geometries. This procedure generated a large number of sterically unfavored interactions between atoms of newly replaced residues. The system was subjected to an energy minimization procedure with the first 100 steps of steepest descent followed by a conjugate gradient minimizer until the convergence criteria of 0.1 kcal/(mol Å) were met. The electrostatic interactions were calculated with a dielectric constant of 4. The protein atoms were treated with the united atom representation, while the atoms in the FAD molecule were calculated with an all-atom force-field (Weiner *et al.*, 1986). Atomic charges for the flavin and the substrate molecules were derived by using the program CHELP (Chirlian & Francl, 1987) on a Cray Y-MP at the Pittsburgh Supercomputing Center. The conditions for the minimization procedure (atomic representations, assignment of atomic charges, dielectric constant, cutoffs for nonbonded interactions, etc.) were at first tested on the structure of MCAD. Atomic coordinates of C_8-CoA, as derived from the crystal structure of the complex between MCAD and C_8-CoA, were placed in the native MCAD structure. When this system was minimized, the conformational changes observed in the resulting structure of substrate-bound MCAD were in good agreement with those observed in the X-ray structure of the MCAD–substrate complex. Details of the modeling procedures will be described elsewhere.

RESULTS AND DISCUSSION

Molecular Model. In the absence of crystallographic data, we modeled human LCAD on the basis of the X-ray crystallographic coordinates of pig MCAD. Superposition of the final minimized model of LCAD onto the minimized X-ray structure of pig MCAD (Figure 2) shows that minor backbone changes were sufficient to accommodate the substituted residues within the core of the molecule. The root mean square deviation for the main-chain atoms, between the LCAD model and the minimized MCAD, is 0.89 Å, whereas the root mean square deviation between the crystal structures of native MCAD before and after the minimization under identical conditions is 0.60 Å. Comparison of the active sites

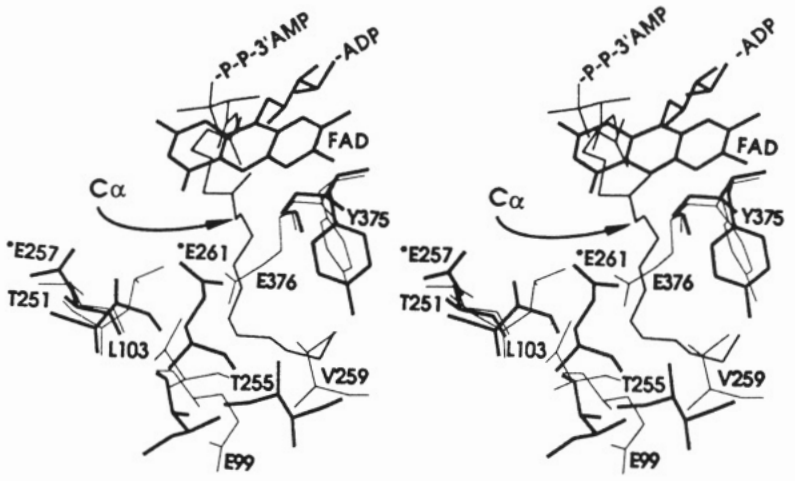

FIGURE 3: Stereoview of the structure of the complex of MCAD and C_8-CoA superimposed on the minimized model of LCAD in the presence of C_{12}-CoA. For clarity, only the residues in the active site that were identified to undergo conformational changes in the complex of MCAD and C_8-CoA (Kim *et al.*, 1993) and the corresponding residues from LCAD are shown. An arrow points to the α-carbon of the substrate that becomes deprotonated by the active site base. LCAD residues are drawn with thick lines; MCAD residues, with thin lines. The numbering corresponds to the MCAD structure except *E257 and *E261, which belong to LCAD corresponding to T251 and T255, respectively, of pig MCAD.

indicates that the carboxylate group of E261 from LCAD (T255 in pig MCAD) lies in the same location as the carboxylate group of glutamate 376 from pig MCAD (G382 in LCAD). However, these two residues belong to two different helices and protrude into the substrate binding pocket forming about a 70° angle between the Cα atom of LCAD E261, the Cα atom of the fatty acyl-CoA substrate, and the Cα atom of MCAD E376. LCAD modeled with C_{12}-CoA or C_{16}-CoA bound to the active site also indicated that E261 was the closest residue to the Cα atom of the fatty acid and was located at approximately the same distance (γ-carboxylate to Cα of C_{12}-CoA, ~4 Å) as E376 in the structure of the MCAD molecule (Kim *et al.*, 1993). A comparison of the active sites between the structure of pig MCAD with C_8-CoA complexed and the minimized model of LCAD in the presence of C_{12}-CoA is shown in Figure 3. E376 from MCAD was previously identified and confirmed as the proton-abstracting base responsible for the first step of the dehydrogenation reaction (Powell & Thorpe, 1988; Bross *et al.*, 1990; Kim *et al.*, 1993). Primary sequence alignment showed that LCAD contains a glycine at the position corresponding to MCAD residue 376; there was no other neighboring glutamate or any other base that would take the role of E376. The three-dimensional model of LCAD suggested that although E261 and E376 are separated by over 100 residues in the primary structure, E261 could effectively replace E376 in a three-dimensional arrangement. The model suggests that E261 of LCAD may correspond to E376 of MCAD as the catalytic residue. Site-directed mutagenesis was then used to test this hypothesis.

Expression of the Active Site Mutant of Human LCAD. The expression plasmids pETLCAD/E261Q and pETLCAD were transformed into *E. coli* strain BL21(DE3). Cotransformation of the cells with plasmid pGroESL, which directs the synthesis of bacterial chaperonin proteins GroES and GroEL, was performed to obtain a high yield of soluble human LCAD. The cells were grown at 30 °C to an optical density of 0.5–0.6 at 600 nm. Expression of human LCAD was induced by addition of 0.1 mM isopropyl 1-thio-β-D-galactopyranoside (IPTG), and the cells were harvested 16 h after the induction. The cells were sonicated, and the soluble fractions of the extracts were subjected to immunoblot analysis using anti-human LCAD antibody. The expression levels, based on the same amounts of total proteins, of both the wild-type and the mutant human LCAD were similar, with an identical subunit molecular mass of 44 kDa for both LCADs (Figure 4). This indicates that the loss of the negative charge introduced by the mutation neither decreases the solubility of the protein nor increases its accessibility to intracellular proteases.

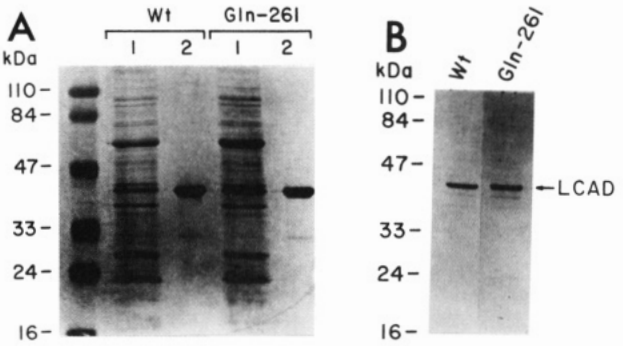

FIGURE 4: SDS–PAGE and Western blot of the wild-type and mutant LCADs. (A) 12% SDS–PAGE. Lanes 1, Wt and Gln-261, contain equal amounts of total protein from cell extracts expressing wild-type and mutant LCAD, respectively. Lanes 2, Wt and Gln-261, contain 2 μg of the purified wild-type and mutant LCADs, respectively. (B) *E.coli* cells transformed with pETLCAD or pETLCAD/E261Q were grown and induced with IPTG. Extracts were prepared, and 20 μg of each of the soluble proteins was separated by a 12% SDS–PAGE and subjected to an immunoblot analysis.

Protein Purification. E261Q mutant LCAD was isolated from large-scale cultures of bacteria using chromatographic techniques. The SDS–PAGE demonstrates high purity (>95%) and an appropriate molecular size of the protein (Figure 4A). We obtained 5–6 mg of pure enzyme per 10 g of wet cell paste. The purification procedure was identical to that used to obtain the wild-type enzyme. The altered enzyme was virtually inactive; therefore, the LCAD-containing fractions were followed on the basis of the elution profiles of the wild-type enzyme, SDS–PAGE, and the A_{280}/A_{450} ratio. The mutant enzyme was indistinguishable from the wild-type enzyme by SDS–PAGE and Western blot analysis, as shown in Figure 4. The protein is relatively stable, although an increased loss of flavin content can be observed after a period of time (2 days at 4 °C). Catalytic assays and spectrophotometric determinations were performed on freshly prepared protein samples that had similar absorption ratios. Turnover

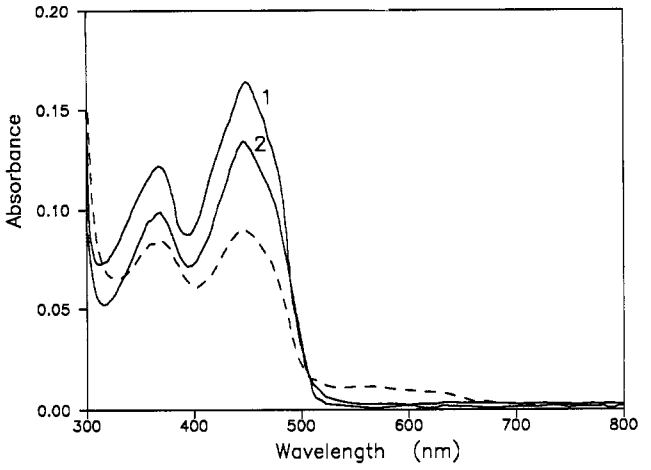

FIGURE 5: Absorption spectra of E261Q and wild-type human LCAD. Curve 1 is the spectrum of the 13 μM mutant LCAD. The dashed curve was obtained immediately after the addition of a 15-fold molar excess of decanoyl-CoA to the 9.7 μM wild-type enzyme, whose spectrum is shown by curve 2.

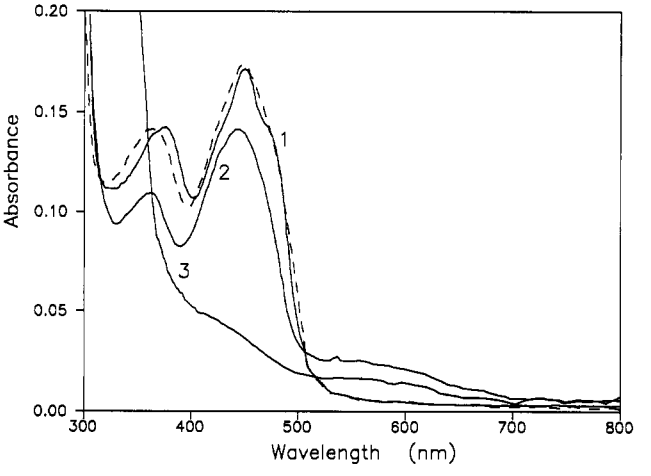

FIGURE 6: Absorption spectra of E261Q human LCAD mutant upon anaerobic addition of C_{10}-CoA. The dashed spectrum (unnumbered) was obtained from purified mutant LCAD (13 μM) in 50 mM potassium phosphate, pH 7.6, and 10% glycerol. Spectrum 1 was obtained 1 h after the addition of a 15-fold molar excess of C_{10}-CoA. This spectrum is identical to the one obtained immediately after substrate addition, and no additional changes were observed after 36 h. Spectrum 2 was obtained in a separate experiment, using the same protein preparation (11 μM), immediately after addition of a 15-fold molar excess of acetoacetyl-CoA, and spectrum 3 was obtained after reduction by sodium dithionite.

numbers were calculated on the basis of flavin concentration using the extinction coefficient of 1.33×10^4 M^{-1} cm^{-1} at 450 nm, for both the wild-type and the mutant enzyme, determined from the visible spectra and amino acid analyses of the purified proteins.

Spectral Properties. The UV–vis spectrum of mutant LCAD shown in Figure 5 is virtually identical to that of the wild-type enzyme and rat liver LCAD. The spectrum exhibits maxima at 275, 371, and 447 nm with absorbance ratios of 7.0:0.8:1.0, respectively. The 447-nm absorbance becomes well resolved upon binding of substrate, exhibiting small shoulders approximately 20 nm on either side of the absorption maximum (Figure 6). The resolved features of the spectrum indicate that flavin lies in a less hydrogen bonding environment in the enzyme–substrate complex (Auer & Frerman, 1980). The crystal structure of the native MCAD (Kim *et al.*, 1993) revealed ordered water molecules in the active site cavity that are displaced by the fatty-acyl moiety of the bound substrate. The similarity between the spectra of the wild-type and the mutant dehydrogenase suggests that the mutant enzyme is properly folded and capable of binding the substrate.

A 15-fold molar excess of decanoyl-CoA (C_{10}-CoA) was anaerobically added to the mutant enzyme, and the spectral changes were followed (Figure 6). Immediately after the addition of the substrate, Michaelis complex formation was detected by about a 3-nm red shift of the absorption maximum and a marked resolution of the 450 nm absorbance. Within a 36-h period, however, no detectable reduction of the flavin 450-nm absorbance was observed by the previously described method used to maintain an anaerobic condition. If the flavin had been reduced by the substrate and quickly reoxidized by oxygen present in the system, a long-wavelength band would appear due to charge-transfer complex formation between the reduced flavin and the enoyl-CoA product. No charge-transfer complex was detected even after 36 h; however, addition of sodium dithionite fully reduced the flavin spectrum (Figure 6). Furthermore, under the experimental conditions, the upper limit of oxygen contamination is less than 2 ppm, corresponding to 90 pmol of O_2 in the volume of the cuvette, 1 cm^3. This amount of oxygen would not be sufficient to reoxidize the 13 nmol of flavin that was present in the experiment, even if the mutant enzyme was more reactive with molecular oxygen compared to the wild type. We have also attempted to determine the rate of flavin reduction with C_{16}-CoA using the procedure described above for C_{10}-CoA. However, at 100 μM concentration of C_{16}-CoA, micelle formation resulted in base-line shifts, causing difficulties in interpreting the results of the experiment (data not shown). Despite the shift of the base line, we have detected formation of a Michaelis complex as exhibited by a spectral red shift accompanied by the appearance of shoulders around the 450-nm peak. Spectral measurements of the wild-type enzyme with C_{10}-CoA clearly showed a decrease in the intensity of the 450-nm peak that was recovered upon the flavin reoxidation (Figure 5).

In another experiment, acetoacetyl-CoA, a dead-end inhibitor of the acyl-CoA dehydrogenases, was added to the mutant enzyme in a 15-fold molar excess. Upon addition of the inhibitor, there was a rapid increase in absorbance at 565-nm, indicating charge-transfer complex formation between the enolate of acetoacetyl-CoA and the oxidized flavin. The results show that mutant LCAD binds acetoacetyl-CoA in deprotonated form analogous to wild-type LCAD (data not shown) and MCAD (McKean *et al.*, 1979). However, since the pK_a of the α-proton in acetoacetyl-CoA (9.45) is more than 7 orders of magnitude lower compared to those in fatty acyl-CoA substrates (Gilbert, 1981), it was not clear whether the deprotonation occurs by the same mechanism as in the wild-type enzyme with acyl-CoA substrates or the enzyme binds to the enol tautomer of acetoacetyl-CoA directly. We have determined the pH dependence of the intensity of the 565-nm absorbance. At pH 6.5 no charge-transfer complex was detected, and at pH 8.0 the intensity of the absorption band was 20–30% higher than that observed at pH 7.6 for both the wild-type and the mutant (data not shown). This pH dependence is consistent with the fact that four-carbon fatty acyl-CoAs are not good substrates and that the charge-transfer complexes observed in both the wild-type and the mutant enzyme are those with the stable enolate form of acetoacetyl-CoA. It should be noted, however, that acetoacetyl-CoA binds to the enzyme despite its short acyl chain length.

Table 1: Specific Activities of Expressed Wild-Type and Mutant Human LCAD

assay	specific activity[a] wild type (wt)	mutant	mutant/wt
PMS + DCPIP	73 ± 9	0.18 ± 0.1	0.002
ETF + DCPIP	25 ± 3		
ferricenium	135 ± 13	0.4 ± 0.17	0.003
ETF fluorescence[b]	186 ± 8	0.028	0.000 15

[a] Specific activity is expressed as a turnover number: (μmol of terminal acceptor)/(μmol of FAD)/min. All of the assays were performed with 50 μM decanoyl-CoA except the ETF-fluorescence assay, which was done using octanoyl-CoA as a substrate. The results are average values obtained with three different enzyme preparations; each assay was run in triplicate and averaged. [b] This assay was done on only one enzyme preparation.

Enzymatic Activity. There was no detectable enzyme activity in the extracts of cells expressing the mutant plasmid, in contrast to a significant activity found in cell extracts expressing the wild-type enzyme. Turnover numbers for the purified wild-type enzyme were comparable with those of pig liver LCAD (Hauge *et al.*, 1956) (Table 1). The specific activity measurements of the purified wild-type and mutant LCAD enzymes show that the E261Q mutant exhibits between 0.02% and 0.3% of the wild-type enzyme activity depending on the assay method employed. Three different enzyme preparations of both the wild-type and the mutant enzyme have been analyzed with different assay methods. The assays including dyes (DCPIP, PMS, ferricenium) were much less accurate and less sensitive than the ETF fluorescence assay, and they exhibited high backgrounds compared to the measured mutant enzyme activity. This may account for the discrepancy in the rates observed in the two type of assays. Turnover numbers were determined for the wild-type enzyme with C_{16}-, C_{10}-, and C_8-CoA (data not shown) using the ferricenium assay. The values were 130, 135, and 135 min^{-1}, respectively, showing that LCAD accepts C_8-CoA, which was used in the ETF fluorescence assay, as a good substrate. Note that the rates determined for one-electron acceptors (ferricenium and ETF fluorescence assay) were approximately double the rate determined for the reduction of DCPIP, which is a two-electron acceptor. An extremely low rate for the mutant enzyme was observed in the assay using ETF and DCPIP; this prevented us from obtaining accurate measurements. The detection of the mutant activity appears to be inconsistent with the observation that there is no detectable decrease in 450-nm absorbance upon the addition of substrate. The reduction of the mutant dehydrogenase flavin was detected at a slow rate only in the presence of another electron acceptor. In the study of Bross *et al.* (1990), the rate of the flavin bleaching, assumed to represent the rate of the α-proton abstraction, for the E376Q mutant of human MCAD was 0.02% of that observed with wild-type pig kidney MCAD. On the basis of the ability to form the Michaelis complex and to form a charge-transfer complex with acetoacetyl-CoA, it is most likely that mutant LCAD is correctly folded, resulting in no significant difference in its K_m value. However, very low reaction rates prevented us from performing a detailed determination of the kinetic parameters.

General Discussion. Previous studies suggest that LCAD binds inhibitors and alternate substrates differently than MCAD and SCAD. For example, 2-octynoyl-CoA binds covalently in the active site of MCAD but not in that of LCAD, although the LCAD is inhibited, but only reversibly (Ankele *et al.*, 1991). Further, the work of Dommes and Kunau (1984) demonstrated that 4-*cis*-decenoyl-CoA is an excellent alternative substrate for MCAD but not for LCAD. Finally, (methylenecyclopropyl)acetyl-CoA irreversibly inactivates MCAD and SCAD but not LCAD (Ikeda & Tanaka, 1990). These findings suggest that the active site geometry of the LCAD is different from that of other acyl-CoA dehydrogenases. This different geometry may be reflected by our data, which indicate that E261 functions as the catalytic base in LCAD, corresponding to E376 in MCAD.

Elimination of base catalysts by site-directed mutagenesis has reduced turnover numbers throughout a considerable range. K258 is the base catalyst in aspartate aminotransferase. The K258A mutant of aspartate aminotransferase (Toney & Kirsch, 1989) retained less than 10^{-6} of the wild-type activity. Similar reductions of turnover numbers have been reported for site-directed mutants of Δ^5-3-ketosteroid isomerase (Kuliopulis *et al.*, 1991) and triosephosphate isomerase (Knowles, 1991). On the other hand, when the active site residue D375 of pig citrate synthase was replaced by a glycine, asparagine, or glutamine, the catalytic power of the enzyme was decreased to 1, 2, or 6% of the wild-type activity, respectively (Alter *et al.*, 1990). The reduction of the activity by 5000-fold observed in the LCAD mutant is within the range found in the systems cited above. Our results from the site-directed mutagenesis, together with the results for MCAD obtained by Bross *et al.*, suggest that E261 is directly involved in the catalysis.

The residual activity associated with the mutant enzyme without the corresponding flavin bleaching upon substrate addition can be the result of several possibilities. A simple explanation may be the presence of the wild-type enzyme due to a possible transcriptional error. Measured reaction rates for the mutant enzyme will then correspond to the trace level of the wild-type enzyme. The 0.015% reduction of the spectral maximum upon the substrate addition could not be detected in such case. The same behavior would be observed if an endogenous *E. coli* dehydrogenase activity was copurified with the LCAD mutant (Overath *et al.*, 1967; Henry & Cronan, 1991). Another explanation is reoxidation of the reduced flavin by trace amounts of molecular oxygen present in the system. As stated in Experimental Procedures, this again is highly doubtful. Although the probability that any of these would happen is extremely low, they cannot be completely excluded as explanations for the observed data. Alternatively, the extremely low activity associated with the purified mutant LCAD could be an intrinsic property of the mutant enzyme. The mutated enzyme exhibits a low reaction rate through a mechanism different from that of the wild-type enzyme. A detailed examination of the active site of the modeled human LCAD structure does not reveal any other residue that might act as a catalytic base located in the range of 4–5 Å from the Cα position of the substrate. However, another glutamate, E257 (about one helix turn away from E261), which is located about 8 Å away from the Cα in the modeled structure, cannot be completely excluded from affecting the water-mediated catalysis. It might be speculated that α-proton abstraction in the E261Q LCAD is thermodynamically unfavored since it is detectable only under the assay conditions when coupled with reoxidation of the dehydrogenase FAD by other electron acceptors. We intend to measure the redox potentials of the FAD in the wild-type and mutant LCADs and the regulation of their redox potentials by substrate binding to determine whether the redox potential is perturbed by this mutation. It should be noted, however, that the positions of the wavelength maxima are similar for the complexes with acetoacetyl-CoA of both the wild-type and the mutant enzyme. Potentiometric

studies of the native and flavin-substituted old yellow enzyme (Stewart & Massey, 1985) have demonstrated a linear relationship between the redox potentials of the chemically modified flavins and the wavelength maxima of the corresponding complexes with phenols. On the basis of these studies it was expected that the wavelength maxima of the charge-transfer complexes would be different for the wild-type and mutant LCADs, if their corresponding redox potentials were different.

Acyl-CoA dehydrogenases probably have evolved from a common ancestor, despite the fact that the catalytic glutamate is not conserved in the primary sequences. Our investigation shows, however, that the glutamate residue is topologically conserved in the three-dimensional structures of the acyl-CoA dehydrogenases. The ancestral gene may have contained both glutamate residues. During evolution, two groups of the dehydrogenases may have diverged from the ancestor gene: one group contains the catalytic glutamate at the position corresponding to E261 (LCAD and possibly IVD), and the other contains the catalytic glutamate at the position corresponding to E376 as in MCAD. An example of catalytic residues that are topologically conserved yet located at different positions within the polypeptide fold is found in the lipase family (Schrag *et al.*, 1992). In these enzymes, the catalytic aspartate, a member of the catalytic triad, is located either in a loop following β-strand 7 or in a loop following β-strand 6. Human pancreatic lipase contains aspartate at both of these positions; however, only one is involved in catalysis.

Recently, crystals of mutant LCAD have been obtained. We are directing our efforts toward the X-ray analysis of the human wild-type and mutant LCAD structures, as well as continuing mutagenesis experiments, to clarify the observed catalytic properties.

ACKNOWLEDGMENT

We thank Dr. David Deerfield II at the Pittsburgh Supercomputing Center for his assistance in the molecular mechanics calculations. This work was supported in part by a grant from the Pittsburgh Supercomputing Center through NIH National Center for Research Resources Cooperative Agreement P41 RR06009.

REFERENCES

Alter, G. M., Casazza, J. P., Wang, Z., Nemeth, P., Srere, P. A., & Evans, C. T. (1990) *Biochemistry, 29*, 7557–7563.

Ankele, K., Melde, K., Engst, S., Bross, P., & Ghisla, S. (1991) in *Flavins and Flavoproteins 1990*, pp 325–328, Walter de Gruyter & Co., Berlin, New York.

Auer, H. E., & Frerman, F. E. (1980) *J. Biol. Chem. 255*, 8157–8163.

Beckman, J. D., & Frerman, F. E. (1983) *J. Biol. Chem. 258*, 7563–7569.

Beinert, H. (1963) *Enzymes 7*, 447–466.

Bradford, M. (1976) *Anal. Biochem. 72*, 248–254.

Bross, P., Engst, S., Strauss, A. W., Kelly, D. P., Rasched, I., & Ghisla, S. (1990) *J. Biol. Chem. 265*, 7116–7119.

Cambillau, C., & Horjales, E. (1987) *J. Mol. Graphics 5*, 174–177.

Chirlian, L. E., & Francl, M. M. (1987) *J. Comput. Chem. 8*, 894–905.

Crane, F. L., Mii, S., Hauge, J. G., Green, D. E., & Beinert, H. (1956) *J. Biol. Chem. 218*, 701–716.

Dommes, V., & Kunau, W.-H. (1984) *J. Biol. Chem. 259*, 1789–1797.

Gilbert, H. F. (1981) *Biochemistry 20*, 5643–5649.

Ghisla, S., Thorpe, C., & Massey, V. (1984) *Biochemistry 23*, 3154–3161.

Ghisla, S., Engst, S., Moll, M., Bross, P., Strauss, A. W., & Kim, J.-J. P. (1992) in *New Developments in Fatty Acid Oxidation* (Coates, P. M., & Tanaka, K., Eds.) pp 127–142, Wiley-Liss, Inc., New York.

Hauge, J. G., Crane, F. L., & Beinert, H. (1956) *J. Biol. Chem. 219*, 727–733.

Henry, M. F., & Cronan, J. E., Jr. (1991) *J. Mol. Biol. 222*, 843–849.

Ikeda, Y., & Tanaka, K. (1990) *Biochim. Biophys. Acta 1038*, 216–221.

Ikeda, Y., Okamura-Ikeda, K., & Tanaka, K. (1985) *J. Biol. Chem. 260*, 1311–1325.

Indo, Y., Yang-Feng, T., Glassberg, R., & Tanaka, K. (1991) *Genomics 11*, 609–620.

Izai, K., Uchida, Y., Ori, T., Yamamoto, S., & Hashimoto, T. (1992) *J. Biol. Chem. 267*, 1027–1033.

Kelly, D. P., Kim, J.-J. P., Billadello, J. J., Hainline, B. E., Chu, T. W., & Strauss, A. W. (1987) *Proc. Natl. Acad. Sci. U.S.A. 84*, 4068–4072.

Kim, J.-J. P., Wang, M., Djordjevic, S., & Paschke, R. (1992) in *New Developments in Fatty Acid Oxidation* (Coates, P. M., & Tanaka, K., Eds.) pp 111–126, Wiley-Liss, Inc., New York.

Kim, J.-J. P., Wang, M., & Paschke, R. (1993) *Proc. Natl. Acad. Sci. U.S.A. 90*, 7523–7527.

Knowles, J. R. (1991) *Nature 350*, 121–124.

Kuliopulis, A., Mildvan, A., & Talalay, P. (1991) *Biochemistry 28*, 149–152.

Lehman, T., & Thorpe, C. (1990) *Biochemistry 29*, 10594–10602.

Matsubara, Y., Indo, Y., Naito, E., Ozasa, H., Glassberg, R., Vockley, J., Ikeda, Y., Kraus, J., & Tanaka, K. (1989) *J. Biol. Chem. 264*, 16321–16331.

Matsubara, Y., Ito, M., Glassberg, R., Satyabhama, S., Ikeda, Y., & Tanaka, K. (1990) *J. Clin. Invest. 85*, 1058–1064.

McKean, M. C., Frerman, F. E., & Mielke, D. (1979) *J. Biol. Chem. 254*, 2730–2735.

Naito, E., Ozasa, H., Ikeda, Y., & Tanaka, K. (1989) *J. Clin. Invest. 83*, 1194–1198.

Nickbarg, E. B., Davenport, R. C., Petsko, G. A., & Knowles, J. R. (1988) *Biochemistry 27*, 5948–5960.

Overath, P., Raufuss, E.-M., Stossel, W., & Ecker, W. (1967) *Biochem. Biophys. Res. Commun. 29*, 28–32.

Powell, P. J., & Thorpe, C. (1988) *Biochemistry 27*, 8022–8028.

Roe, C. R., & Coates, P. M. (1989) in *The Metabolic Basis of Inherited Disease* (Scriver, C. R., Beaudet, A. L., Sly, W. S., & Valle, D., Eds.) pp 889–914, McGraw-Hill, New York.

Schrag, J. D., Winkler, F. K., & Cygler, M. (1992) *J. Biol. Chem. 267*, 4300–4303.

Stewart, R. C., & Massey, V. (1985) *J. Biol. Chem. 260*, 13639–13647.

Thorpe, C., Ciardelli, T. L., Stewart, C. T., & Wieland, T. (1981) *Eur. J. Biochem. 118*, 279–282.

Toney, M. D., & Kirsch, J. F. (1989) *Science 243*, 1485–1488.

Weiner, P. K., & Kollman, P. A. (1981) *J. Comput. Chem. 2*, 287–303.

Weiner, S. J., Kollman, P. A., Case, D. A., Singh, V. C., Ghio, C., Alagona, G., Profeta, S., Jr., & Weiner, P. (1984) *J. Am. Chem. Soc. 106*, 765–784.

Weiner, S. J., Kollman, P. A., Nguyen, D. T., & Case, D. A. (1986) *J. Comput. Chem. 7*, 230–252.

Williamson, G., Engel, P. C., Mizzer, J. P., Thorpe, C., & Massey, V. (1982) *J. Biol. Chem. 257*, 4314–4320.